JAST, Vol. 13, No. 1, pp. 26-38

JAST
Journal of Aerospace Science and Technology

Scientific-Research Article

9DoF Modeling of Parafoil with Transverse Displacement of Payload

Meghdad Torabi Nejhad [1], Fariborz Saghafi [2]*

1 , 2 Engineering Faculty of Aerospace, Sharif Technical University

* Azadi Street Tehran, Iran

Email: * saghafi@sharif.edu

Parafoil-payload system, as a complex system, is used widely today and has various usages. This system is a multibody complex whose components, have dynamic interactions and relative movements. The present study deals with the multibody modeling and simulation of nine degrees of freedom flight dynamics of a parafoil-payload system, which includes six degrees of translational and rotational freedom of parafoil set (parachute and ropes), and three degrees of relative rotational freedom of the payload. By kinematic and dynamic analysis of the system components, a nonlinear model with 18 state variables is obtained. This model has three controlling inputs. In addition to symmetric and asymmetric aerodynamic brakes, the shifting of the weight of the payload with respect to the parafoil is considered, which leads to the deflection and change of the transverse installation angle of the parachute with respect to the parafoil set. The apparent mass and moment of inertia of the parafoil parachute, restraining forces, relative movements between objects, longitudinal and transverse installation angles and also the effect of wind are examined. In order to evaluate how the flight dynamics of the system work and the study of the factors affecting it, the nonlinear differential equations of the model are developed. After examining its stability using Lyapanov method, the model undergoes a numerical integration as well as simulation for several flight conditions and under different inputs by the code and program developed in MATLAB software. The simulation results show the flight stability that is achieved after launching from a high altitude and by which the flight dynamic modeling of the system is validated.

Key words: *multibody modeling, dynamic analysis of parafoil-payload system, flight simulation*

Introduction

Flight dynamics of the parafoil-payload system are different than those of a conventional airplane. In other words, the large distance between the aerodynamic center of the parachute and the center of mass of the whole system, the relative movements between the components of the system and the presence of apparent mass will lead to this difference. Due to the joint between the parafoil and the payload, these two objects have independent relative movements. Therefore, the parafoil-payload system should be considered as a multibody set.

Depending on degrees of freedom (2 to 12), taking into account the relative movements between the components of the system, each model has different specific purpose and level of accuracy. In most references, the model with 6 degrees of freedom, which includes three degrees of translational and three degrees of rotational freedom has been used to

1 Msc
2 Associate Professor (corresponding author)

Received Date: 20 Feb. 2020
Accepted Date: 20 May 2020

design guidance and control algorithms. Article [4] uses dynamic model of 8 degrees of freedom (including six degrees of freedom of parafoil movement and two degrees of relative freedom of movement of the payload) with the purpose of software developing for a modeling and simulation most compatible with reality. Reference [5] examines the dynamic model of 9 degrees of freedom, six degrees of rotational and transfer freedom of the parafoil and three degrees of rotational freedom of the payload. This article, regarding the shape of the parachute as a set of interconnected panels and also using defined aerodynamic coefficients, provides reasonable control responses to right and left brake shifts and longitudinal installation angles. Article [7], by simply introducing the shifting weight of the payload in the parafoil control of a 6-degree-of-freedom model, has investigated various influential factors such as the distance of the payload to the parachute wing. Article [8] also discusses the use of transverse installation angle in guiding and controlling a 6-degree-of freedom model of the parafoil-payload system.

In the mentioned articles, the angles of longitudinal and transverse installation, apparent mass and place in which it applies, transverse displacement of the weight of the payload with respect to the parafoil frame and wind flow are not directly used in extracting the equations. In the present paper, assuming the longitudinal installation angle of the parachute wing is constant, a control mechanism at the junction between the parafoil and the payload is considered so that the payload will have a transverse displacement relative to the center of the mass of the parafoil. This distribution, which is accompanied by a shift in the length of the ropes attached to the parachute wing, causes a change in the uniform distribution of the mass of the payload in the ropes from the initial state. This control mechanism actually plays a role in guiding and transverse control of the system as an alternative to asymmetric brake movement. The present work, developing the relations related to the effect of the apparent mass and determining the place in which it applies, tries to develop more accurate equations of dynamic models, contrary to previous works, which, to simplify, have considered the apparent mass as a single point on the aerodynamic center or on the center of the parafoil mass. This paper, using a 9-degree-of-freedom dynamic model, starts with the multibody modeling of the system, and, after linearization and the study of the stability of the model, analyzes the flight dynamic behavior of the parafoil-payload system by providing some examples of dynamic responses. It needs to mention that the equations and symbols are written according to the standards given in the reference [9].

According to Figures 1 and 2, the parafoil-payload system is modeled as a parachute wing with a fixed (rigid) shape that has two symmetry plates xz and yz and is connected to the payload by means of ropes connected to it, through joint c. This model includes six degrees of rotational and translational freedom of the parafoil and three degrees of rotational freedom of the payload relative to the parafoil. Parafoil (parachute wings and the ropes attached to it) and the payload rotate freely around the joint (gimbal type), relative to each other. In this model, using a control mechanism, the joint has a transverse displacement to the parafoil, which leads to the displacement of the weight of the payload relative to the parafoil set. This system consists of two main frames, parafoil and payload, which their base triads are located in the centers of mass of parafoil and payload, points S and B, respectively. The parachute wing frame and the related triad are located at point A, the aerodynamic center of the parachute wing. To express the orientation of the parachute wing frame relative to the parafoil, the coordinate system (]P) of the parachute, in terms of longitudinal Γ and lateral Λ installation angles, parafoil body coordinate system (]B), to express the orientation of the parafoil frame relative to the inertial reference frame (]I), according to Euler roll angles φB, the pitch θB, and yaw ψB, the inertial coordinate system that acts as an interface and fixed coordinate system at the point c. The payload Coordinate System (]S), to express the orientation of the payload frame relative to inertia, in terms of the relative Euler angles of the roll φ S, picth θ S, and Yaw ψ S, the aerodynamic coordinate system (]A), arising from the relative wind around, with the aid of the angle of attack αB and the sideslip of βB, is associated with the parachute wing coordinate system. The Wind coordinate system (W) which is connected to the inertia coordinate system by angles of inclination η and azimuth μ. The transfer matrices of the parachute with respect to the parafoil coordinate systems [T] PB, the aerodynamic with respect to the parachute coordinate systems [T] AP, and the wind with respect to the inertia coordinate systems [T] WI are given in Equations 1, 2, and 3. For short, instead of cos and sin functions, the symbols C and S with the corresponding lower case are used, respectively.

$$[T]^{PB} = \begin{bmatrix} C_\Gamma & 0 & -S_\Gamma \\ S_\Lambda S_\Gamma & C_\Lambda & S_\Lambda C_\Lambda \\ C_\Lambda S_\Gamma & -S_\Lambda & C_\Lambda C_\Gamma \end{bmatrix} \quad (1)$$

$$[T]^{AP} = \begin{bmatrix} C_{\alpha_a} C_{\beta_a} & S_{\beta_a} & S_{\alpha_a} C_{\beta_a} \\ -C_{\alpha_a} S_{\beta_a} & C_{\beta_a} & -S_{\alpha_a} S_{\beta_a} \\ -S_{\alpha_a} & 0 & C_{\alpha_a} \end{bmatrix} \quad (2)$$

$$[T]^{WI} = \begin{bmatrix} C_\eta C_\mu & C_\eta S_\mu & -S_\eta \\ -S_\mu & C_\mu & 0 \\ S_\eta C_\mu & S_\eta S_\mu & C_\eta \end{bmatrix} \quad (3)$$

The transfer matrices between each of the parafoil and the payload body with respect to the inertia coordinates, [T] BI and T] SI, respectively, are generally expressed as Equation 4 matrices, except that the parafoil and payload Euler angles must be placed in this matrices.

$$\begin{bmatrix} C_\theta C_\psi & C_\theta S_\psi & -S_\theta \\ S_\varphi S_\theta C_\psi - C_\varphi S_\psi & S_\varphi S_\theta S_\psi + C_\varphi C_\psi & S_\varphi C_\theta \\ C_\varphi S_\theta C_\psi + S_\varphi S_\psi & C_\varphi S_\theta S_\psi - S_\varphi C_\psi & -C_\varphi C_\theta \end{bmatrix}$$

Geometric and mass characteristics of the model

Geometric and mass characteristics of the model include parafoil specifications: span length b, chord length C, parachute wing curvature a, parachute wing thickness t, parachute wing reference area SP, rope length R, parachute mass mC, and payload specifications: payload mass mS , the payload reference area SS, length xS, width yS and height zS of the payload are listed in Table 1.

Table 1. The Geometric and Mass Characteristics of the Parafoil-payload system

m_c (kg)	R (m)	S_p (m^2)	t (m)	a (m)	c (m)	b (m)	
5	6.6	28.49	0.67	1.16	3.7	7.7	Parafoil
-	-	z_s (m)	y_s	x_s	s_s	m_s	
-	-	0.7	0.5	0.7	0.5	140	Payload

The position vector of the center of the mass of the payload relative to the joint C expressed in the payload coordinates, the position vector of the center of rotation of the parachute wing T relative to the center of the mass of the parafoil B expressed in the parafoil body coordinate, the position vector of the aerodynamic center A relative to the center of rotation of the parachute in the parachute wing coordinate system, and the position vector C relative to the center of rotation of the parachute expressed in the parafoil body coordinate system are shown as [ssc]s = [0 0 0.5]T, [sTB]B= [00 -0.58]T, [sAT]P= [0.925 0 0]T, and $[s_{CT}]^B = [0L6.481]^T$, respectively. L is the transverse displacement of the C joint, which is performed by the corresponding control mechanism. The changes of this displacement are in the form of Equation 5.

$$L = k_L (U_L - L)\ ,\ at\ t = 0 \rightarrow L = 0 \quad (5)$$

In this case, U_L is the input and K_L is a constant value that depends on the type of operator used. The changes of the transverse installation angle Λ are also proportional to L and are obtained from Equation 6.

$$\dot{\Lambda} = \dot{L}/(s_{CT})_3 \times \cos^2 \Lambda \quad ,(s_{CT})_3 = 6.481 \quad (6)$$

In this model, the longitudinal installation angle is considered Γ = −9 deg.

Aerodynamic characteristics of the model

Aerodynamic coefficients of drag force C_{Dp}, lateral force C_{YP}, and lift force C_{LP} , according to the reference 6 (pages 25 and 26), are considered as lookup tables for a similar parafoil. The aerodynamic coefficients of the roll moment ClP, pitch CmP, and yaw CnP, which are considered as the normal relations of a flying vehicle, are considered according to the reference [10]; they have been omitted here for the sake of brevity.

Multi-body modeling of parafoil-payload system

In order to model the system, the Newton-Euler method was used, which is performed by developing kinematic equations, transfer and position dynamics for the payload and the parafoil as well as the constraint equations between them. The set of nonlinear equations consists of 18 state variables, which has the general form of relation 7. These equations represent a completely complex and coupled system. In this regard, X are the state variables and U are the control inputs.

$$\dot{X} = f(X,U)$$
$$X = \left\{ [s_{BI}]^I, [v_B^I]^I, [\omega^{BI}]^B, [\omega^{SI}]^S, \frac{d}{dt}\Theta_B, \frac{d}{dt}\Theta_S \right\}$$
$$U = \{\delta_s, \delta_a, U_L\}$$

In the relation 7, $[S_{BI}]^I$ and $[v^I B]^I$ are the displacement vector and the inertia velocity of the parafoil in the inertia coordinate system, respectively. $[\omega^{BI}]^B$ and $[\omega^{SI}]^S$ are the angular velocity vectors of the parafoil and the payload relative to the inertial frame in their preferred coordinate systems. ΘB and ΘS are matrices of Euler angles of the parafoil and the payload, respectively. δ_s and δ_a are symmetric and asymmetric displacement of aerodynamic brakes,

and u_L is also related to the transverse displacement of the payload weight relative to the parafoil.

The Kinematics of the parafoil-payload system

The translational and rotational kinematic equations of the system are as follows:

$$\left[\frac{d}{dt}s_{BI}\right]^I = \left[v_B^I\right]^I$$

$$\frac{d}{dt}\Theta_B = \begin{bmatrix} 1 & \sin\phi_B\tan\theta_B & \cos\phi_B\tan\theta_B \\ 0 & \cos\phi_B & -\sin\phi_B \\ 0 & \sin\phi_B/\cos\theta_B & \cos\phi_B/\cos\theta_B \end{bmatrix}\left[\omega^{BI}\right]^B$$

$$\frac{d}{dt}\Theta_S = \begin{bmatrix} 1 & \sin\phi_S\tan\theta_S & \cos\phi_S\tan\theta_S \\ 0 & \cos\phi_S & -\sin\phi_S \\ 0 & \sin\phi_S/\cos\theta_S & \cos\phi_S/\cos\theta_S \end{bmatrix}\left[\omega^{SI}\right]^S$$

The parafoil equations

The parafoil equations include kinematic and dynamic equations of translation and rotation. With the development of kinematic relations, the relation of translaional acceleration of the parafoil is obtained in the body coordinate system as follows.

$$\left[a_B^I\right]^B = \left[a_{C_B}^I\right]^B - 2\left[\Omega^{BI}\right]^B\left[\frac{d}{dt}s_{C_BB}\right]^B \cdots$$
$$+\left[S_{C_BB}\right]^B\left[\frac{d}{dt}\omega^{BI}\right]^B - \left[\Omega^{BI}\right]^B\left[\Omega^{BI}\right]^B\left[s_{C_BB}\right]^B$$

In the relation 9, $[a^I_{CB}]^B$,$[\ \Omega^{BI}]^B$, and $[\ S_{CBB}]^B$ are the Inertial translational acceleration of the joint C, the skew-symmetric matrix of Parafoil angular velocity vector, and the skew-symmetric form of the position vector of the joint relative to the mass center of the parafoil in the parafoil coordinate system, respectively.

Due to $\left[\frac{d}{dt}\ s_{TB}\right] = 0$,we have:

$$\left[\frac{d}{dt}s_{C_BB}\right]^B = \left[\frac{d}{dt}s_{C_BT}\right]^B + \left[\frac{d}{dt}s_{TB}\right]^B = \begin{bmatrix} 0 \\ \dot{L} \\ 0 \end{bmatrix}$$

According to the forces exerted on the parafoil, the Newtonian relation and also the relation 9, the translational dynamic equation of the parafoil will be as follows:

$$m^B\left[a_B^I\right]^B = m^B[T]^{BI}[g]^I + \left[\overline{T}\right]^{PB}\left[F_{p-aero}\right]^P \cdots$$
$$+\left[F_{app}\right]^B + [T]^{BI}\left[F_B\right]^I$$

In the relation 11, m^B and $[g]^I$ show the parafoil mass and the gravity rate in the inertial coordinate system. $[F_B]^I$ represents the inertial constraint force of the connection junction in the inertial coordinate system, which is exerted from payload to the parafoil. The aerodynamic forces in the parachute coordinate system are as follows:

$$\left[F_{p-aero}\right]^P = \bar{q}_P S_p\left[\overline{T}\right]^{AP}\begin{bmatrix} -C_{D_p} \\ C_{Y_p} \\ -C_{L_p} \end{bmatrix}$$

In this relation, the dynamic pressure q_P is as follows:

$$\bar{q}_P = \frac{1}{2}\rho\left|v_A^{wind}\right|^2$$
$$\left[v_A^{wind}\right]^P = \left[v_A^I\right]^P - [T]^{PW}\left[v_{wind}^I\right]^W \ ,\ [T]^{PW} = [T]^{PI}\left[\overline{T}\right]^{WI}$$

$[v^I{}_A]^p$ and $[v^{wind}{}_A]^P$ are the speed of the aerodynamic center relative to the inertial frame and the speed of the aerodynamic center relative to the relative wind in the parachute coordinate system, respectively. $[v^I{}_{wind}]^W$ is the wind speed relative to inertial frame in the wind coordinate system.

The apparent force $[F_{app}]^B$ exerted on the parachute wing, which in fact originates from the apparent mass, is obtained by the rotational derivative of the apparent linear moment with respect to the inertial frame in the parafoil body system as follows:

$$\left[F_{app}\right]^B = -\left[D^I p_{app}\right]^B$$
$$,\left[p_{app}\right]^B = [M_F]\left[v_{M_i}^{wind}\right]^B = [M_F]\left(\left[v_B^I\right]^B - \left[v_{wind}^I\right]^B\right) \cdots$$
$$-[M_F]\left[S_{M_iB}\right]^B\left[\omega^{BI}\right]^B \quad for\ i = 1,2$$
$$\Rightarrow \left[F_{app}\right]^B = -[M_F]\left(\left[\frac{d}{dt}v_B^I\right]^B + \left[\Omega^{BI}\right]^B\left[v_{wind}^I\right]^B\right) \cdots$$
$$-[M_{a\Omega}]\left[\frac{d}{dt}\omega^{BI}\right]^B - \left[\Omega^{BI}\right]^B\left[P_{app}\right]^B$$
$$,[M_{a\Omega}] = -[M_F]\left[S_{M_iB}\right]^B = \begin{bmatrix} 0 & m_x z_{M_1} & 0 \\ -m_y z_{M_2} & 0 & 0 \\ 0 & 0 & 0 \end{bmatrix}$$
$$,[M_F] = \begin{bmatrix} m_x & 0 & 0 \\ 0 & m_y & 0 \\ 0 & 0 & m_z \end{bmatrix},\quad \left[S_{M_iB}\right]^B = \begin{bmatrix} 0 & -z_{M_1} & 0 \\ z_{M_2} & 0 & 0 \\ 0 & 0 & 0 \end{bmatrix}$$

In the relation 14, considering the form 2, m_x is the apparent mass in the first direction of the parafoil body system, located at the apparent mass center of M_1, m_y and m_z, also, are the apparent masses in the second and third directions of the parafoil coordinates, located in the center of the apparent mass of m_2, respectively. Z_{m1} and z_{m2} are the vertical distances of the apparent mass centers relative to the center of the mass of the parafoil. $[s_{m1B}]^B$ is the antisymmetric matrix of the position vector of

apparent mass centers relative to the parafoil mass center in the parafoil body system. For the sake of brevity, the equations m_x, m_y, m_z, z_{m1} and z_{m2} are not mentioned. How to obtain these quantities are mentioned in the reference 1.

Considering the moments applied to the parafoil and by the Euler relation, the attitude dynamic equation of the parafoil is as follows:

$$\left[I_B^B\right]^B\left[\frac{d}{dt}\omega^{BI}\right]^B+\left[\Omega^{BI}\right]^B\left[I_B^B\right]^B\left[\omega^{BI}\right]^B=$$
$$\left[\overline{T}\right]^{PB}\left[M_{p-aero}\right]^P+\left[M_{app}\right]^B+\left[S_{C_BB}\right]^B[T]^{BI}\left[F_B\right]^I\ldots$$
$$+\left[\overline{T}\right]^{PB}\left[S_{AB}\right]^P\left[F_{p-aero}\right]^P+[T]^{BI}\left[M_B\right]^I$$

In this relation, $[I^B_B]^B$ is the inertia moment matrix in the parafoil body system. $[S_{CBB}]^B$ and $[S_{AB}]^P$ are the skew-symmetric matrices of the position vector of the joint relative to the center of parafoil mass in the parafoil system, and the skew-symmetric matrix of the position vector of the aerodynamic center relative to the center of mass of the parafoil in the parachute coordinate system, respectively.

$[M_B]^I$ is the inertial constraint moment which is applied to the parafoil through the joint. The aerodynamic moment in the parachute coordinate system $[M_{p\text{-}aero}]^P$ is obtained according to the roll, pitch, and yaw moment coefficients as equation 16:

$$\left[M_{p-aero}\right]^P=\bar{q}_PS_P\begin{bmatrix}bC_{l_P}\\cC_{m_P}\\bC_{n_P}\end{bmatrix}$$

The apparent moment $[M_{app}]^B$ is obtained through the rotational time derivative of the apparent angular moment $[h_{app}]^B$ relative to the inertia frame in the parafoil body system as follows:

$$\left[M_{app}\right]^B=-\left[D^I h_{app}\right]^B$$
$$,\left[h_{app}\right]^B=[I_F]\left[\omega^{BI}\right]^B+\left[S_{M_iB}\right]^B\left[p_{app}\right]^B=[I_{a\Omega}]\left[\omega^{BI}\right]^B\ldots$$
$$+[I_{av}]\left(\left[v_B^I\right]^B-\left[v_{wind}^I\right]^B\right)\quad for\ i=1,2$$
$$\Rightarrow\left[M_{app}\right]^B=-[I_{a\Omega}]\left[\frac{d}{dt}\omega^{BI}\right]^B\ldots$$
$$-[I_{av}]\left(\left[\frac{d}{dt}v_B^I\right]^B+\left[\Omega^{BI}\right]^B\left[v_{wind}^I\right]^B\right)-\left[\Omega^{BI}\right]^B\left[h_{app}\right]^B$$
$$,[I_{a\Omega}]=\left[S_{M_iB}\right]^B[M_{a\Omega}]+[I_F],\quad[I_{av}]=\left[S_{M_iB}\right]^B[M_F]$$
$$,[I_F]=\begin{bmatrix}I_{app-x}&0&0\\0&I_{app-y}&0\\0&0&I_{app-z}\end{bmatrix}$$

In the relation 17, $I_{app\text{-}x}$, $I_{app\text{-}y}$, and $I_{app\text{-}z}$ are apparent inertia moments in the direction of the first, second, and third axes of the parafoil body coordinate system. How to obtain them is mentioned in the reference 1.

The equations of the payload

The payload equations include kinematic and dynamic relations. The translational acceleration of the payload mass center in the payload coordinate system $[a^I_S]^S$ is obtained as follows:

$$\left[a_S^I\right]^S=-\left[S_{SC_S}\right]^S\left[\frac{d}{dt}\omega^{SI}\right]^S+\left[\Omega^{SI}\right]^S\left[\Omega^{SI}\right]^S\left[s_{SC_S}\right]^S+\left[a_{C_S}^I\right]^S$$

$[S_{SCS}]^S$ and $[\Omega^{SI}]^S$ are skew-symmetric matrices of the position vector of the payload mass center relative to the joint C and the angular velocity vector of the payload frame relative to the inertia in the payload machine, respectively. $[a^I_{Cs}]^S$ is the inertial translational acceleration of the joint in the coordinate system of the payload.

The translational dynamic equation of the payload is as follows:

$$m^S\left[a_S^I\right]^S=m^S[T]^{SI}[g]^I+\left[F_{s-aero}\right]^S+[T]^{SI}\left[F_S\right]^I$$

M^s and $[F_S]^I$ are the mass of the payload and the internal constraint force in the inertial coordinate system, which is applied to the payload through the joint. The aerodynamic force applied to the payload is calculated as follows, in terms of the drag coefficient of the payload:

$$\left[F_{s-aero}\right]^S=\bar{q}_SS_S\begin{bmatrix}-C_{D_S}\\0\\0\end{bmatrix},\quad\bar{q}_S=\rho/2\left|v_S^{wind}\right|^2$$

The wind speed relative to the payload $[v^{wind}{}_S]^S$ is thus obtained:

$$\left[v_S^{wind}\right]^S=\left[v_S^I\right]^S-[T]^{SI}\left[v_{wind}^I\right]^I$$

Using the Euler relation, the attitude dynamic equation of the payload in the payload coordinate system using the moments applied to it:

$$\left[I_S^S\right]^S\left[\frac{d}{dt}\omega^{SI}\right]^S+\left[\Omega^{SI}\right]^S\left[I_S^S\right]^S\left[\omega^{SI}\right]^S=$$
$$\left[S_{C_SS}\right]^S[T]^{SI}\left[F_S\right]^I+[T]^{SI}\left[M_S\right]^I$$

$[I^S_S]^S$ and $[S^I_{CsS}]^S$ are the moment of inertia of the payload and the skew-symmetric matrix of the position of the joint C relative to the center of mass of the payload in the payload coordinate system, respectively. $[M_S]^I$ is the constraint moment applied to the payload through the joint.

Constraint equations

According to Figure 1, the two objects are connected to each other by a virtual link. At the junction of this link to two bodies (C_S and C_B), the constraint forces F_B and F_S and moments M_B and M_S are applied to each of these objects. A total of six equations of constraint are considered. These equations that are dependent on the type of the joint and degrees of the freedom of the system, are as follows:

$$[F_B]^I = -[F_S]^I = [F_I]^I \ , \ [F_I]^I \neq [0]$$
$$[M_S]^I = -[M_B]^I = [0] \ , \ \left[S_{C_B C_S}\right]^I [F_I]^I = [0]$$
$$\left[\frac{d}{dt} v^I_{C_B}\right]^I - \left[\frac{d}{dt} v^I_{C_S}\right]^I = [0]$$
$$\left[\frac{d}{dt} \omega^{BI}\right]^I - \left[\frac{d}{dt} \omega^{SI}\right]^I \neq [0]$$

Investigating the stability of a dynamic model

Lyapunov linearization method is used to evaluate the model stability. This method relates to the local stability of a nonlinear system. Considering the relation 7, by equating the derivatives of state variables to zero and solving equations in the form of (X, U)= 0, the equilibrium point (x_*, u_*) is obtained. Expanding the tailor series of the relation 7, we will have:

$$\dot{x} = \left(\frac{\partial f}{\partial x}\right)_{(x_*,u_*)} x + \left(\frac{\partial f}{\partial u}\right)_{(x_*,u_*)} u + f_{h.o.t}(x,u)$$

Omitting the aforementioned sentences $f_{h.o.t}(x, u)$ and defining Jacobi matrices, we have:

$$A = \left(\frac{\partial f}{\partial x}\right)_{(x_*,u_*)} \qquad B = \left(\frac{\partial f}{\partial u}\right)_{(x_*,u_*)}$$
$$\Rightarrow \dot{x} = Ax + Bu$$

The eigenvalues of matrix A are as follows:

$$\begin{Bmatrix} 0,0,0,-12.9430,-0.3560,-0.0006, \\ -0.1508 \pm 8.1176i, -0.1013 \pm 2.4331i, \\ -0.7902 \pm 7.3144i, -4.2142 \pm 4.1779i, \\ -0.1706 \pm 0.6058i, 0, 0 \end{Bmatrix}$$

As can be seen, there are 5 eigenvalues of zero. These eigenvalues are related to inertial displacements and Euler's two yaw angles of the parafoil and the payload. In fact, these eigenvalues are related to state variables that their values has no influence on the system dynamics. Regardless of these eigenvalues, other eigenvalues are in the left half side of the complex plane; therefore, this nonlinear system is stable at equilibrium point.

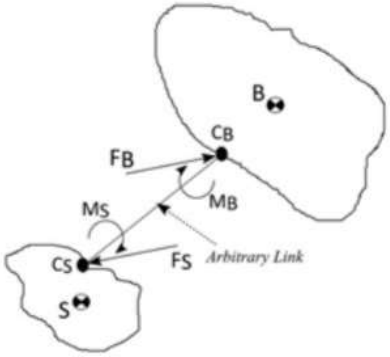

Figure 1- The parafoil-payload system as a two-bodies system

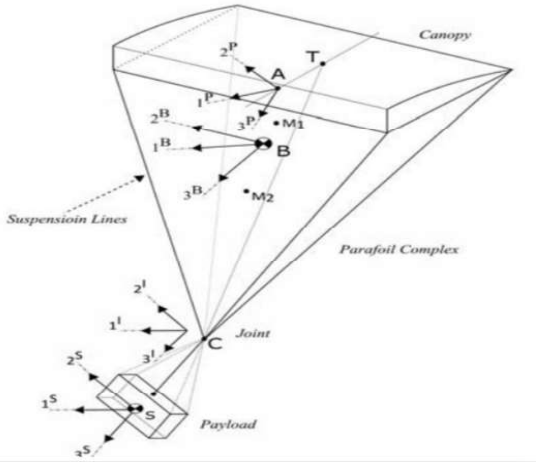

Figure 2- Schematic pattern of the parafoil-payload system

Simulating the model

In order to validate the flight dynamics modeling, the model is solved and simulated by the fifth-order Runge Kutta integration method with a time

constant of 0.01 seconds. The initial conditions of the model are as follows:

$$u_0 = 13.71\ m/s,\ \ w_0 = 2.51\ m/s,\ \ z_0 = 1000\ m$$
$$\theta_{B_0} = -4.294\ \text{deg},\ \ \theta_{S_0} = -0.0174\ \text{deg}$$

It is worth noting that the other state variables are considered zero at the initial moment.

Model response to symmetrical displacement of the aerodynamic brake

In this condition, after a 5-second trim flight, the input δ_s , with a delay time of one second, is displaced in two different states for 30 seconds, and then returns to the previous state (δ_s=0) with a delay of one second. According to the figure 3, for δ_s= 45, the parafoil pitch angle reaches -8.29 degrees after about two oscillations from the initial value of -4.29 degrees and returns to its original equilibrium value by returning the input to zero value. For δ_s= 90, θ_B , after two oscillations and more dramatic changes between -15/2 and 7/2 degrees, reaches -7/54, and then returns to the original equilibrium value when the input is zero. The payload also experiences pitch angle fluctuations. When the input is given, θ_s also experiences a fluctuation between -14/4 to 16/2, but then returns to its initial value when the input is zero. As observed, with the rise of the displacement of the input δ_S, pitch angle fluctuations increase in both parafoil and payload. The figure 4 shows the height changes according to the system range. By the rise of δ_S , due to the reduction of the ratio L/D (aerodynamic efficiency), the head angle is increased, which reduces the forward distance and also due to the reduction of the vertical component of parafoil velocity, the rate of descent decreases; figure 5 also displays parafoil angle of attack changes.

With the displacement of δ_s, the angle of attack αB, through some fluctuations, reaches 8/2 degrees from the initial value of 10/39, and then returns to its original equilibrium point when the input is zero. With the rise of the input to 90 degrees, the fluctuations of the angle of attack also increase and finally return to the initial value after reaching the value of 32.11 degrees. Normally, this input is applied during landing and deceleration (flare flight phase).

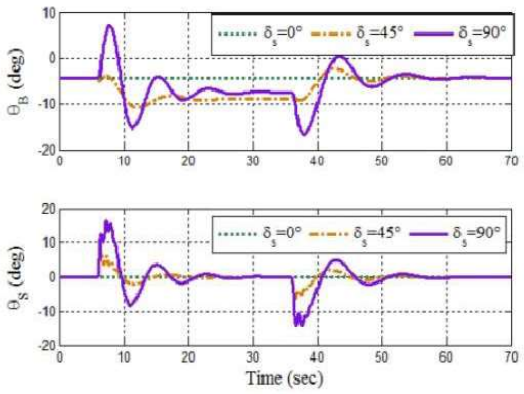

Figure 3 – Variation of the parafoil and payload roll Euler angles in reponse to delts

Figure 4- Height changes in terms of range in respone to delts

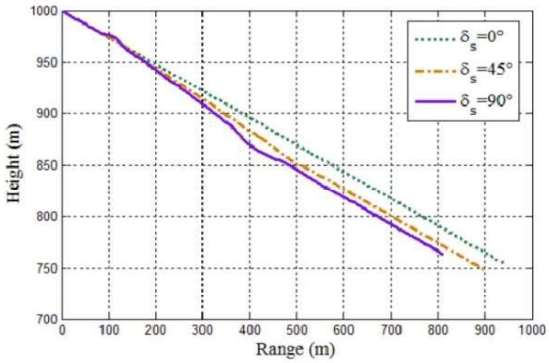

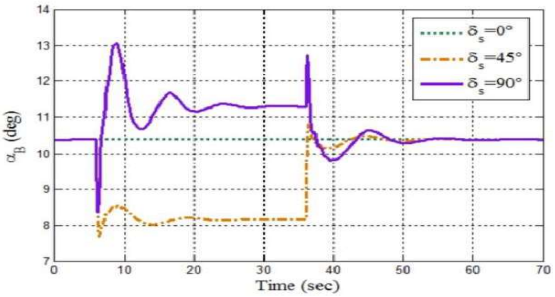

Figure 5- Change in the parafoil angle of attack

Model response to asymmetric displacement of aerodynamic brakes

In this state, after a 25-second trim flight, δ_a, with a delay of a second, moves for two positions. Figure 6 shows the variations of the Euler roll and yaw of the parafoil. When δ_a equals 45 degrees, the roll angle φB reaches the final value 16 from the initial value zero. By increasing δ_a to 90 degrees, the parafoil rolling oscillation increases to 30.2 degrees; also, the parafoil takes more direction angle and changes direction to the right. In other words, in this

situation, the parafoil skids more during the bypass maneuver. Due to the lateral and longitudinal dynamics, the lateral slip and parafoil angle of attack change and deviate from their original value. The figure 7 shows these changes. As observed, the increase of δ_a leads to the rise in the oscillations of installation angles α_B and β_B and in the 90-degree-displacement position, they reach the final values of 0.5 degrees and 6.13 degrees, respectively. Figures 8 and 9 show three-dimensional path and lateral distance changes in terms of range. As observed, the increase in δ_a displacement is followed by a decrease in rotation radius during the maneuver and consequently the rotation rate increases and the system decreases the altitude at a higher rate.

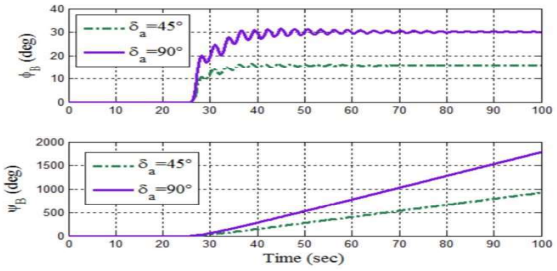

Figure 6- Changes in the parafoil Euler roll and yaw angles in reponse to delta

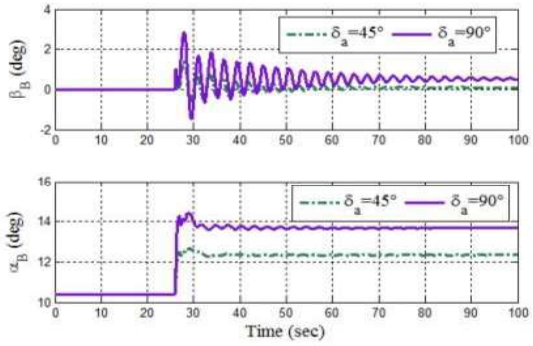

Figure 7- Changes in sideslip and parafoil angles of attack in respose to delta

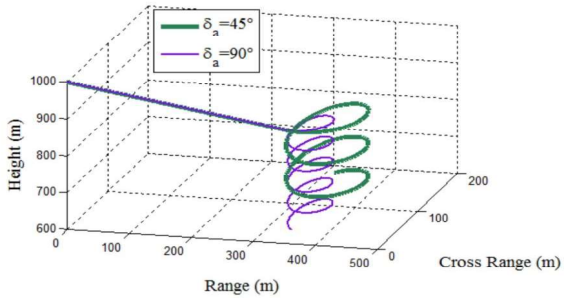

Figure 8- The three-dimensional path of the system in response to delta

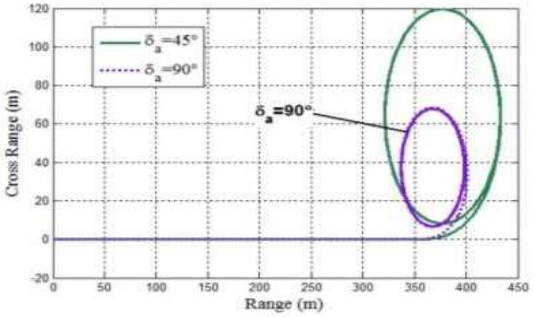

Figure 9- Changes of the lateral distance in terms of range in response to delta

Model response to transverse displacement of payload weight

Relative to parafoil

As mentioned in the introduction, transverse displacement of the payload weight relative to the parafoil can be used as an alternative to asymmetric brake displacement. Figure 10 shows the temporal variations of the transverse displacement of the c joint due to two different UL inputs. In the relation 5, KL is considered 0/7. The figure 11 shows the changes in lateral distance in terms of range in response to these two inputs mentioned. As observed, the system has done the S or 8 maneuver in response to the inputs. The second entrance, in which the transverse displacement changes in the range of -0.25 to 0.25 m, has led to a maneuver with a smaller turning radius and a higher rate. Figure 12 shows the Euler roll, parafoil pitch and yaw angle shifts in response to these inputs. By moving the joint to the right and disturbing the initial transverse equilibrium, as well as restoring this equilibrium by the parachute wing, a negative roll torque is created in the parafoil, which leads to a negative Euler roll angle (φB) . By changing the direction of displacement of the joint to the left, a positive roll torque and a positive bank angle are created. As the parafoil rolls and the aerodynamic forces deflect, the pitch also changes so that it shifts. The joint to the right becomes more negative and by changing the direction of movement to the left, first by making a positive and then negative oscillation, and finally by zeroing the input, θ returns to its original value of the trim. Changes in the yaw angle are similar to the roll angle, first negative and then positive.

In other words, by moving the joint to the right, the system rotates to the left and vice versa. Also according to the figure 12, by increasing the

transverse displacement of the payload, the range of response changes of the system also increases.

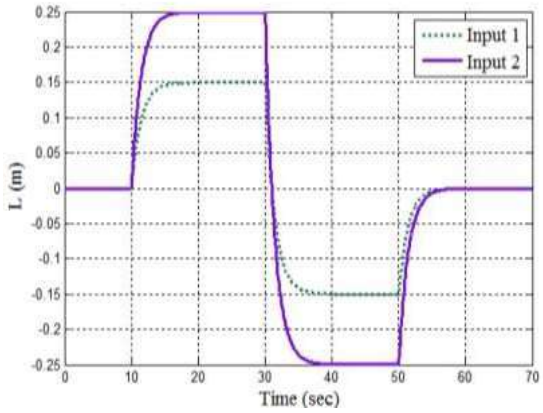

Figure 10- Changes of the transverse displacement the joint C relative to parafoil

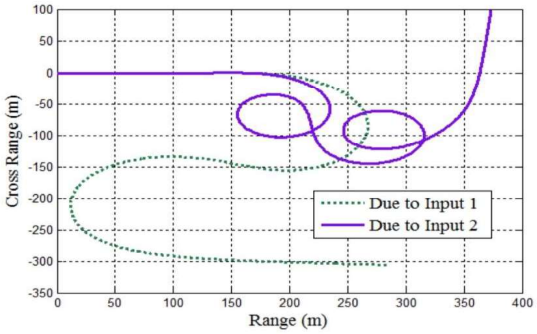

Figure 11- Changes of the lateral distance displacement in terms of range in response to two inputs of UL

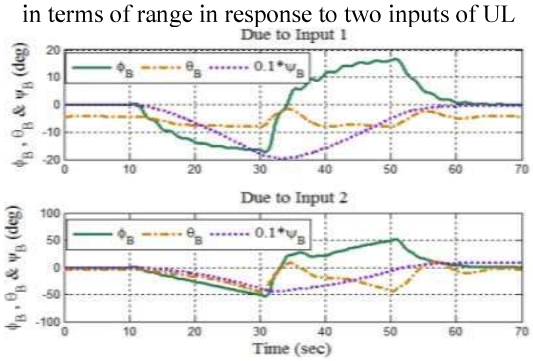

Figure 12- Changes of the parafoil Euler angles in Response to two inputs of UL

Investigation of the effect of apparent mass and moment of inertia

In this section, by applying input similar to Section 2-5 to the model, the following four conditions are considered. Case 1: The real model consists of apparent force and momentum and two centers of apparent mass. The second case: the model without considering the apparent force and moment. Third case: the model includes apparent force and momentum, but assuming that the center of the second apparent mass of M2 is in place of M1. Case 4: The model includes the apparent force and momentum, but assuming that both apparent mass centers are located at the location of the parafoil mass center. Figure 13 shows the height changes in terms of range and figure 14 shows the partial magnification shown in the final phase for the 4 mentioned states.

As can be seen, in the second case the radius of rotation is larger than in the first case, but the rate of reduction of height is lower. The third case (simplified model 1) is more in line with the real model than the others. The fourth mode (simplified model 2) also has a smaller turning radius than the real model but is almost the same with the rate of height reduction.

Figure 13- Height Changes in Terms of Range, Apparent Mass Effect Investigation

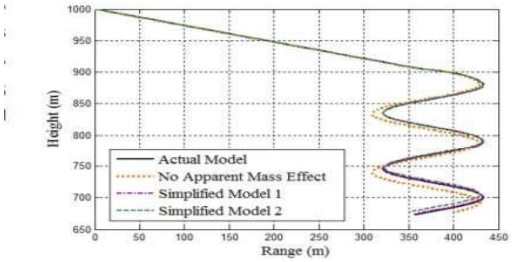

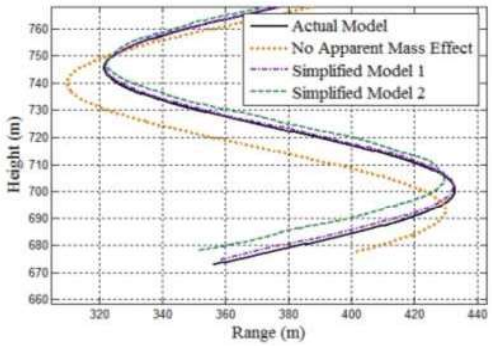

Figure 14- Figure 13 Magnification, Apparent Mass Effect Investigation

Investigation of effect of wind

In this section, two modes are considered. Case 1: From the beginning, the system, without any input, is exposed to the continuous model of Drayden turbulent wind flow. The standard used in this model

is MIL-F-8785C. The figure 15 shows Euler angles time shifts. As can be seen, these angles fluctuate around the range of their trim value. The figure 16 also shows the three-dimensional path for the two cases: one considering the wind current, and the other excluding it. The second case: The system, after a 25-second flight without the wind current, without any input, is exposed to wind from the rear at a speed of 4 meters per second, with the elevation and azimuth angles of $\eta = -45$ deg. and zero, which then changes to $\mu = 20$ deg. after a flight to the 6oth second. The figure 17 shows the parafoil Euler angles shifts in this case. In the 25th second, only the pitch angle fluctuates, which returns to its original value after about 25 seconds. In the 60th second when the system is exposed to lateral wind, all three angles of position fluctuate and change due to the coupling of the lateral and longitudinal dynamics; the difference is that the roll and yaw angles fluctuate more sharply than the pitch angle. In this case, the heading angle of the system changes and deviates to the right (east). The angles of attack and sideslip of the parafoil also increase due to changes in the translational velocity; figure 18 shows these changes.

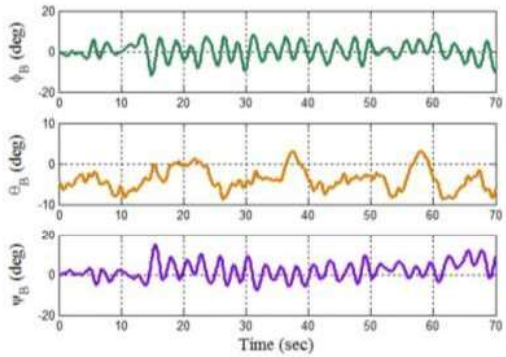

Figure 15- Changes of the parafoil Euler angles, Phase 1

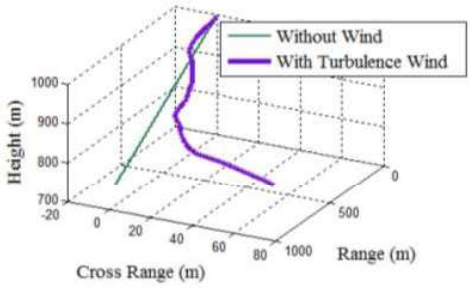

Figure 16- The three-dimensional path of the parafoil, Phase 1

Figure 19 shows the three-dimensional path of the system in this case. According to the figure, first the system increases the sideslip angle and then in the 60th second, by being exposed to the lateral wind flow from the left, it changes direction to the right (east). Due to the dynamic interaction between the parafoil and the payload, the payload, the same as the parafoil, changes position. Figure 20 shows the time variations of the Euler's angles of the payload. In the 60th second, all three angles oscillate; With the difference that the start of the pitch angle fluctuations at this moment is much less than in the 25th second. Due to the type of connection joint and the absence of bounded directional momentum, the Euler angle of the payload begins to increase at 60s.

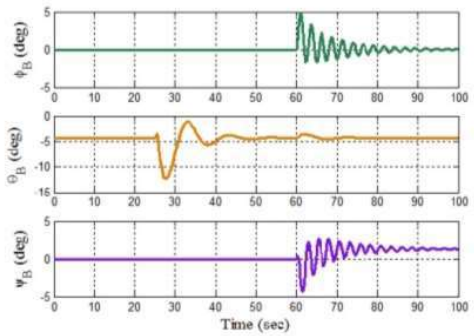

Figure 17- Changes of parafoil Euler angles, Phase 2

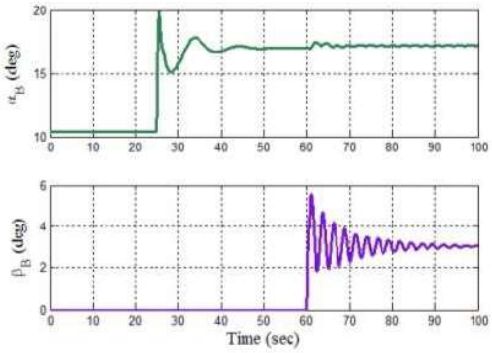

Figure 18- Changes of parafoil sideslip and angle of attack , Phase 2

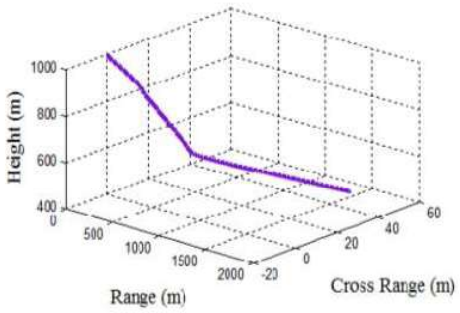

Figure 19-The parafoil three-dimensional path, Phase 2

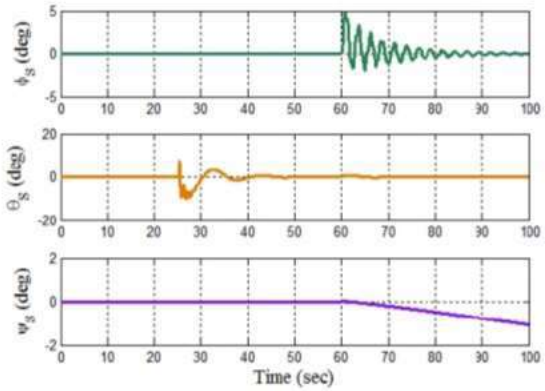

Figure 20- Changes of payload Euler angles, Phase 2

Conclusion

This paper deals with multi-body modeling of a dynamic model of 9 degrees of freedom of a parafoil-payload system. Using Newton-Euler method and developing the dynamic relations as well as considering constraint equations, a set of relations indicating the dynamic behavior of the model was obtained. After review stability and the effect of symmetric and asymmetric aerodynamic brake inputs and transverse displacement of payload weight with respect to parafoil, apparent mass and moment of inertia and its places of application and wind flow were investigated with. The following results were obtained: 1. Symmetrical aerodynamic brake input increases sideslip angle and decreases descent rate, therefore, it can be used for smooth and controlled descent. 2.The asymmetric aerodynamic brake input, which is used to perform lateral maneuvers, can be used to control the route and steer to the desired destination. In this case, due to the coupling, the longitudinal dynamics also changes. 3. Transverse displacement of the payload weight relative to the parafoil changes the transverse installation angle of the parachute wing frame relative to the parafoil, which can be considered as an alternative to asymmetric braking for maneuvering. 4. Places of apparent mass are located at two separate points relative to the center of mass of the parafoil, which must be considered for more accurate modeling. 5. Wind flow, including sudden and accidental winds, in addition to changing the aerodynamics, changes the apparent moments and forces, which will lead to a change in the behavior of the system.

References

[1] Kowaleczko, G., "Apparent masses and inertia moments of the parafoil," Journal of Theoretical and Applied Mechanics, 52, 2014.
[2] Devalla, V. and Prakash, O., "Developments in unmanned powered parachute aerial vehicle: a review,"IEEE Aerosp Electron Syst Mag 2014;29(11):6–20.
[3] Sun H, Sun Q and Luo S, "In-flight compound homing methodology of parafoil delivery systems under multiple constraints," Aerosp Sci Technol 2018;79:85–104.
[4] Heise, M. and Muller, S., "Dynamic Modeling and Visualization of Multi-Body Flexible Systems," AIAA Modeling and Simulation Technologies Conference and Exhibit, Providence, Rhode Island, August 2004.
[5] Slegers, N. and Costello, M., "Aspects Of Control For a Parafoil and Payload System," Journal of Guidance, Control and Dynamics, 2003.
[6] Prakash, O. and Ananthkrishnan, N., "Modeling and Simulation of 9-DOF Parafoil-Payload System Flight Dynamics," AIAA 2006-6130.
[7] Ward, M. and et al, "Parafoil Control Using Payload Weight Shift," AIAA 2012-4738.
[8] R. Haji Babaei and F. Saghafi, Using the Angle of Installation of the Parachute Wing in the Guidance and Control of the Parafoil-Payload System, 14th International Conference of the Iranian Aerospace Association, Tehran
[9] Zipfel, P.H., Modeling and Simulation of Aerospace Vehicle Dynamics, Second Edition, University of Florida, 2007.
[10] Lingard, J.S., "Ram-Air Parachute Design," 13th AIAA Aerodynamic Decelerator Systems Technology Conference, May 1995.
[11] Slotine, J.E. and Li, W., Applied Nonlinear Control, Prentice Hall, 1991.